PROTEINS: Structure, Function, and Genetics 44:484–489 (2001)

Quantum Mechanics Simulation of Protein Dynamics on Long Timescale

Haiyan Liu,[1,2,5] Marcus Elstner,[3,4] Efthimios Kaxiras,[3] Thomas Frauenheim,[4] Jan Hermans,[2] and Weitao Yang[1]*

[1]*Department of Chemistry, Duke University, Durham, North Carolina*
[2]*Department of Biochemistry and Biophysics, University of North Carolina, Chapel Hill, North Carolina*
[3]*Department of Physics, Harvard University, Cambridge, Massachusetts*
[4]*Department of Theoretical Physics, University of Paderborn, Paderborn, Germany*
[5]*School of Life Science, University of Science and Technology of China, Hefei, China*

ABSTRACT **Protein structure and dynamics are the keys to a wide range of problems in biology. In principle, both can be fully understood by using quantum mechanics as the ultimate tool to unveil the molecular interactions involved. Indeed, quantum mechanics of atoms and molecules have come to play a central role in chemistry and physics. In practice, however, direct application of quantum mechanics to protein systems has been prohibited by the large molecular size of proteins. As a consequence, there is no general quantum mechanical treatment that not only exceeds the accuracy of state-of-the-art empirical models for proteins but also maintains the efficiency needed for extensive sampling in the conformational space, a requirement mandated by the complexity of protein systems. Here we show that, given recent developments in methods, a general quantum mechanical-based treatment can be constructed. We report a molecular dynamics simulation of a protein, crambin, in solution for 350 ps in which we combine a semiempirical quantum-mechanical description of the *entire* protein with a description of the surrounding solvent, and solvent-protein interactions based on a molecular mechanics force field. Comparison with a recent very high-resolution crystal structure of crambin (Jelsch et al., Proc Natl Acad Sci USA 2000;102:2246–2251) shows that geometrical detail is better reproduced in this simulation than when several alternate molecular mechanics force fields are used to describe the entire system of protein and solvent, even though the structure is no less flexible. Individual atomic charges deviate in both directions from "canonical" values, and some charge transfer is found between the N and C-termini. The capability of simulating protein dynamics on and beyond the few hundred ps timescale with a demonstrably accurate quantum mechanical model will bring new opportunities to extend our understanding of a range of basic processes in biology such as molecular recognition and enzyme catalysis. Proteins 2001;44:484–489.** © 2001 Wiley-Liss, Inc.

Key words: protein structure; quantum mechanics; molecular dynamics simulation; structural accuracy

INTRODUCTION

Computer simulation of the structure and dynamics of proteins and other biological macromolecules based on empirical potential energy functions [molecular mechanics (MM)] has become a widely used tool in the last two decades.[1–3] Although such studies have been insightful, the use of quantum mechanical (QM) models to complement MM-based studies has been pursued for a number of reasons.

One reason to use a QM model is to achieve higher accuracy. In general, the functional forms and parameters in empirical MM models are optimized to reproduce a certain set of experimental or theoretical data, the latter from accurate quantum mechanical calculations. The accuracy of a MM model is thus limited not only by its empirical functional form but also by the amount and the accuracy of the data used in the parameterization process. The accuracy achieved with MM simulations varies, depending on the type of molecular systems and on the property of interest.

In general, QM models produce more complicated and more realistic potential energy surfaces than MM models, and the first-principle nature of QM models implies broader transferability. The accuracy of many currently popular MM models is limited by important factors, such as absence of charge transfer interactions and environment-dependent polarization effects, which are included in QM models.

Probably the most important reason for using a QM model is to simulate chemistry involving electronic structure changes that are not described by MM models. The development of QM/MM models, which treat a small part of a macromolecular system by QM and the rest by MM, has brought about the capability to simulate chemical processes in enzymatic systems.[4–6] The limitation inher-

Grant sponsor: Center for Research Resources, National Institutes of Health; Grant number: RR08102; Grant sponsor: National Science Foundation: Grant number: CHM-9730962.

*Correspondence to: Jan Hermans, Department of Biochemistry and Biophysics, University of North Carolina, Chapel Hill, NC 27599-7260 or Weitao Yang, Departmnt of Chemistry, Duke University, Durham, NC 27708-0348. E-mail: hermans@med.unc.edu or yang@chem.duke.edu

Received 9 April 2001; Accepted 27 April 2001

ent in conventional QM models of being able to treat only a small part of the system by QM sometimes results in arbitrary partitioning of the QM and MM subsystems and nonphysical treatment of the bonded boundary between the subsystems. Frequently, this limitation is accompanied by inconsistent treatment of interactions within different partitions and across partitions. Linear-scaling approaches allow for larger QM subsystems,[7] and the consequent extension of the size of the QM partition can greatly reduce the errors resulting from the approximations in a QM/MM model.

In this work, we developed a linear-scaling semiempirical quantum mechanics-based approach aiming at long timescale molecular dynamics simulation of proteins, and this quantum mechanical model is applied to an entire protein molecule. The approach we constructed has the following key features: (a) a hybrid quantum mechanical/molecular mechanical scheme[4–6] that allows use of an explicit solvation model without an increase of the size of the quantum mechanical system; (b) the divide-and-conquer approach[7,8]; (c) an efficient and accurate self-consistent-charge density functional theory-based tight-binding scheme (SCC-DFTB)[9,10]; and (d) the explicit incorporation of the long-range van der Waals energy and forces left out by the quantum mechanical model.

Simulations of crambin in water solution with periodic boundary conditions were conducted on the above potential energy surface [denoted as QMV(P)/MM(S), 350 ps] and also on two other types of potential energy surface: hybrid quantum mechanics/molecular mechanics *without* explicit van der Waals forces between protein atoms [QM(P)/MM(S), 60 ps] and pure molecular mechanics (MM, 350 ps each), in the form of three popular MM force fields for proteins, amber,[11] cedar,[12,13] and charmm.[14] The accuracy of the results is assessed by comparison with a recent very high resolution structure of crambin.[15]

MATERIALS AND METHODS

Implementation of QM-MM

For the protein/water interactions, we follow the QM/MM model first proposed by Warshel and Levitt.[4] The total Hamiltonian of the system is given by

$$H_{\text{total}} = H_{\text{QM}} + H_{\text{MM}} + H_{\text{QM/MM}} \quad (1)$$

where H_{QM} is the Hamiltonian of protein, H_{MM} is the Hamiltonian of solvent (water), and $H_{\text{QM/MM}}$ describes protein/solvent interactions. For protein we used the SCC-DFTB model,[9,10] whereas for solvent we used the TIP3P empirical molecular mechanics model.[16] $H_{\text{QM/MM}}$ consists of electrostatic interactions modeled by including the point charges in the TIP3P water model in the QM calculations of the protein and van der Waals interactions modeled by the sum of atomic Lennard-Jones interactions between protein and water.

The SCC-DFTB Method

The SCC-DFTB scheme can be derived by a second-order expansion of the density functional theory (DFT) total energy functional with respect to the charge density fluctuations $\Delta\rho$ around a given reference density ρ_0.[9,10] This fluctuation is approximated as a difference between atom-centered point charges, $\Delta q_\alpha = q_\alpha - q_\alpha{}^0$, where $q_\alpha{}^0$ is the reference charge of atom α, and q_α is the charge estimated from a Mulliken charge analysis on the basis of the electron density. In a linear combination of atomic orbital (LCAO) representation, the approximate total energy functional is given by

$$E_{tot} = \sum_{i}^{occ} \sum_{\mu\nu} c_\mu^i c_\nu^i H_{\mu\nu}[\rho_0] + E_{rep}[\rho_0] + \frac{1}{2} \sum_{\alpha\beta} \Delta q_\alpha \Delta q_\beta \gamma_{\alpha\beta}. \quad (2)$$

Application of the variational principle to this total energy expression results in a Kohn-Sham equation that needs to be solved self-consistently for the charge fluctuations.

In the SCC-DFTB scheme, ρ_0 is taken as the superposition of pseudoatomic densities from atomic DFT calculations. The values of $H_{\mu\nu}[\rho_0]$ for pairs of atomic elements as functions of interatomic distances are precalculated by using first-principle DFT theory with generalized gradient approximation (GGA)[17] in a two-center approximation using a minimal basis of atomic-like wave functions $\{\phi_\mu\}$.

At long distances between atoms α and β, the third term in the total energy expression represents the Coulomb interactions between the charge fluctuations on them. At shorter distances the exchange-correlation contributions come in, and a rigorous treatment is not possible. An approximation to the on-site term $\gamma_{\alpha\alpha}$ is made on the basis of the derivative of the energy of the highest occupied atomic orbital with respect to its occupation number. An analytical approach is then used to derive an expression for $\gamma_{\alpha\beta}$. As has been pointed out in the original SCC-DFTB paper, there is no adjustable or empirical parameter in the determination of $H_{\mu\nu}[\rho_0]$ or $\gamma_{\alpha\beta}$.

The second term in Eq. 2 represents the repulsive potential. In the SCC-DFTB model, this is represented by a sum of short-range, pairwise interaction energies that depend only on the interatomic distances and that are determined by systematically changing the structure of suitable, small reference molecules and comparing the DFT-GGA energies with the SCC-DFTB electronic energies of these structures. The derivation of this pair-interaction energy for hydrocarbons has been described by Porezag et al.,[18] and recently, the procedure has been described for interactions of sulfur, with as references the molecules S_2H_2, S_2O, SO_2, $S(CH_3)_2$, S_2C, SH_2, and SN_2 computed at the B3LYP/6-31G* level.[19]

Protein System

The starting structure is the 0.83 Å crystal structure of crambin[20] (PDB identification 1ab1). To remove internal stress this structure was energy-minimized to root-mean-square gradient below 1.0 kcal/(mol Å) with the SCC-DFTB model before solvation. Before starting each of the protein simulations, the water molecules were equilibrated on the corresponding potential energy surface by 50 ps simulations.

Computational Details

The divide-and-conquer approach[7,8] has been used to solve the QM problem in the QM(P)/MM(S) and QMV(P)/MM(S) calculations. In the divide-and-conquer calculations, the buffer sizes used for the second row and for the third row elements are 4 Å and 5.5 Å, respectively (the fact that the SCC-DFTB model uses compacted atomic orbital basis functions allows for smaller buffer sizes than previous divide-and-conquer calculations based on the MNDO type model). The buffer regions were updated every 5 MD steps. In the SCC-DFTB calculations, the SCF convergence criteria are that energy converges to $<10^{-6}$ atomic units and that at least four SCF iterations must be performed per step. The SCF calculation was performed at every MD step. After the starting step, the number of SCF iterations at each step rarely exceeded four to satisfy the energy criterion.

The real space Ewald summation is truncated at 13 Å, the reciprocal space summation truncated when $|k| > 8$, and the convergence parameter κ is 0.25. The total potential energies calculated by using these parameters deviate <0.5 kcal/mol from the converged results, or 0.00006 kcal/mol per atom. The van der Waals interactions are calculated by using a twin range cutoff method with a short-range cutoff of 13 Å and a long-range cutoff of 14 Å. To avoid considering every pair of atoms at each step, a group-based pair list at a cutoff of 14 Å updated every 10 steps has been used to calculate the real space Ewald summation and the short-range van der Waals interactions. The MD time step was 1 fs, and all bonds involving hydrogen atoms were constrained by using the shake algorithm.[21]

The temperature of the system was coupled to external baths at 300 K by the weak coupling method,[22] solute and solvent coupled separately. The above protocol led to stable molecular dynamics simulation: a coupling time of 1 ps is sufficient to maintain the correct temperature, and the root-mean-square differences of total, potential, and kinetic energies between successive MD steps are 0.16, 9.4, and 9.4 kcal/mol, respectively.

In one of the two QM-MM simulations [denoted QMV(P)/MM(S)], long-range van der Waals interactions, of the form $-C_6/r_{ij}^6$, where r_{ij} is the interatomic distance and C_6 a coefficient that depends on the atom types, have been explicitly included, with C_6 coefficients taken from the amber force field. To capture only the long-range $1/r^6$ behavior of the van der Waals interactions and to switch off the unwanted $1/r^6$ behavior at shorter distances, where the quantum mechanical model becomes appropriate, a damping function is applied, of the form[23]

$$f_d(r_{ij}) = \{1 - \exp[c(r_{ij} - r_v)^m]\}^n \quad (3)$$

where the van der Waals radius r_v from the amber force field is used. The values used for the parameters in the empirical damping function are $c = -0.9891$, $m = 4$, and $n = 3$. For a pair of sp^3 carbon atoms at a 5.5 Å distance, the undamped $-C_6/r^6$ term gives -0.0223 kcal/mol, the full Lennard-Jones term, C_{12}/r^{12}–C_6/r^6 gives -0.0211 kcal/mol, whereas the damped $-C_6/r^6$ term gives -0.0214 kcal/mol.

TABLE I. Root-Mean Square Deviations (RMSD) From the Starting Crystal Structure in the QMV(P)/MM(S) and MM Simulations (in Å)

Force field	Instantaneous deviation[a]	All atoms[b]	Backbone[c]
QMV(P)/MM(S)	1.21	0.86	0.61
Amber	0.99	0.71	0.48
Cedar	1.05	0.82	0.74
Charmm	1.19	0.95	0.80

[a]Time average of the instantaneous RMSD.
[b]RMSD of the time-averaged structure for all non-hydrogen atoms.
[c]RMSD of the time-averaged structure for backbone atoms (N, C^α, C, and O).

Three separate MM simulations of crambin have been performed by using the same setup as in the QM simulation. The simulation with the amber force field[11] has been performed by using the TINKER program package with a self-implemented Ewald-summation routine. The simulation with the cedar[12,13] and charmm[14] force fields have been performed by using the Sigma program package, which incorporates Darden's particle/mesh Ewald summation code.[24]

RESULTS AND ANALYSIS

Crambin

We find the QMV(P)/MM(S) simulation to accurately maintain the overall experimental structure of crambin,[15] as is also true of the simulations with MM force fields. The instantaneous root-mean-square deviation (RMSD) from the crystal structure fluctuates between 1.0 and 1.5 Å after an initial growth period of ≈20 ps. The averaged RMSDs of the QMV(P)/MM(S) and the three MM simulations are compared in Table I.

Although the QMV(P)/MM(S) simulation is accurate and stable over 350 ps, the 60-ps QM(P)/MM(S) simulation is not, the RMSD from the crystal structure reaching 2.5 Å and continuing to increase. A major defect after the QM(P)/MM(S) simulation is that the two originally α-helical regions of crambin have partially transformed into 3–10 helices.

Helical Oligopeptides In Vacuo

The energy of N-acetyl-$(Ala)_n$-N′-methylamide molecules of different length, $n = 2$, 3, 5, and 8, constrained in either the right-handed α-helical conformation ($\phi = -57°$, $\psi = -47°$) or the 3–10 helical conformation ($\phi = -60°$, $\psi = -30°$) was evaluated with a variety of quantum mechanics methods. The geometries were optimized with the B3LYP/6-31G* model, and single-point energy calculations at both the Hartree-Fock (HF) and MP2 level with the same basis set were performed with these geometries to compare the energy gaps between the two conformations. SCC-DFTB calculations with and without the damped van der Waals term were also conducted on these geometries (Table II). The results obtained with the highly accurate MP2 method

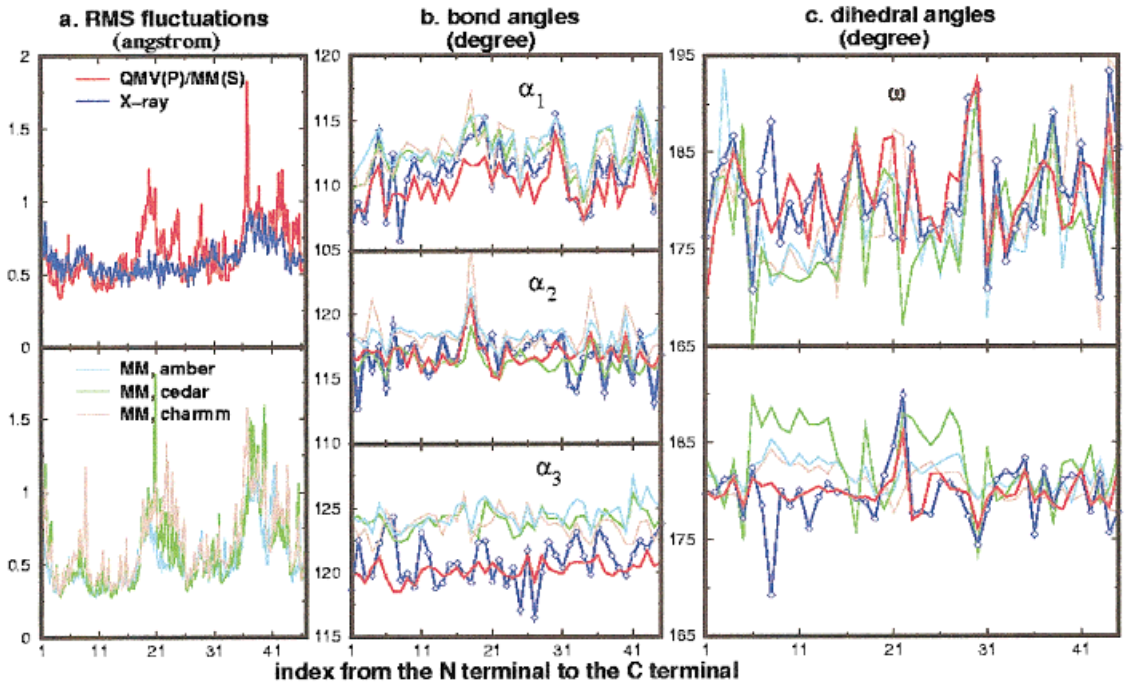

Fig. 1. **a:** Root-mean-square fluctuations of positions of backbone atoms (N, C^{α}, C, and O) observed within the last 300 ps of the QMV(P)/MM(S) and MM simulations (the latter with, respectively, the amber, cedar and charmm force fields) and derived from the crystallographic temperature factors. **b:** Backbone bond angles from the 0.54 Å resolution crystal structure[15] and from the simulations. α_1, α_2, and α_3 correspond to the N_i-C_i^{α}-C_i, C^{α}-C_i-N_{i+1} and C_i-N^{i+1}-C_{i+1}^{α} angles, respectively, where *i* is residue index. **c:** Two dihedral angles related to the planar geometry of peptide units, from the crystal structure and from the simulations (top: C_i^{α}-C_i-N_{i+1}-C_{i+1}^{α} or ω, bottom: C_i^{α}-C_i-N_{i+1}-O_i). The same color scheme is used throughout.

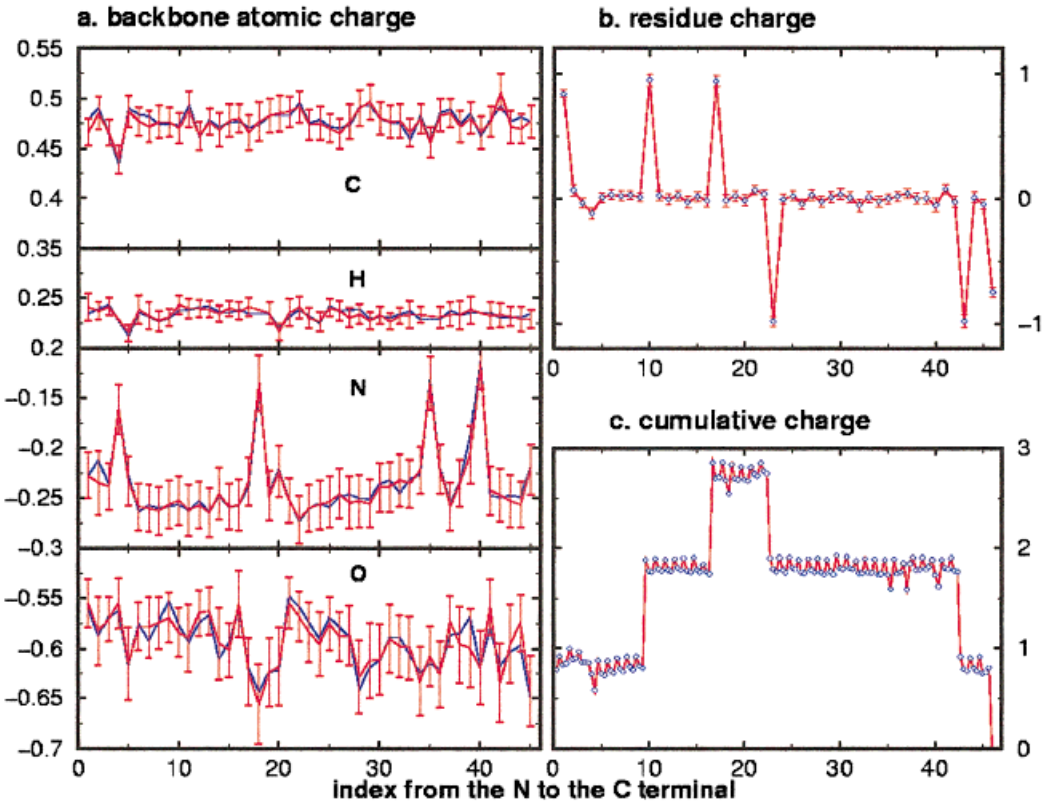

Fig. 2. **a:** Atomic charges on polar backbone atoms (C, O, N, and H) averaged over the 50–200 ps (red) and 200–350 ps (blue) periods of the QMV(P)/MM(S) simulation. The error bars indicate the root-mean-square fluctuations observed during the first 150 ps period. **b:** Averaged net charges on individual amino acid residues with fluctuations. **c:** Cumulative charge along the peptide chain, starting from the N-terminal; the points represent the accumulated value up to each of the three main-chain atoms (N, C^{α}, and C).

TABLE II. Energy Differences (in kcal/mol) Between α and 3–10 Helical Conformations of N-Acetyl-(L-Alanyl)$_n$-N′-Methylamide Molecules

No. of alanine residues	MP2	HF	B3LYP	SCC-DFTB	SCC-DFTB with explicit van der Waals energy
2	3.5	3.3	3.6	2.9	2.9
3	4.8	5.4	4.9	3.8	3.3
5	5.1	7.6	6.3	5.2	3.3
8	2.6	8.9	6.1	5.9	1.4

can be understood by considering that the 3–10 helical conformation is favored by an additional hydrogen bond, whereas long-range interactions favor the more compact α-helix and progressively stabilize the α-helix as the number of alanine residues increases beyond a few. The trend observed with MP2 is captured qualitatively by the SCC-DFTB method when explicit long-range attractive van der Waals forces are included. These results confirm the need to include the long-range attraction explicitly when representing biological macromolecules with all but the highest levels of quantum-mechanics.

Analysis of Geometric Detail

Two observations result from comparison of the QMV(P)/MM with the MM simulations. The first is that the differences between the resulting dynamics are subtle but significant, as indicated by the backbone atom root-mean-square fluctuations [Fig. 1(a)], which show only qualitative agreement among the solution simulations.

The second observation is that the QMV(P)/MM simulation leads to better agreement with the crystal structure of crambin at 0.54 Å resolution for several key peptide backbone geometric parameters, as shown by Figures 1(b) and 1(c). Specifically, the MM simulations are found to produce systematic deviations for the main-chain bond angles. Averages both over time and along the chain, are $\angle\ N_iC_i^{\alpha}C_i = \alpha_1 = 111.2°$, $\angle\ C^{\alpha}C_iN_{i+1} = \alpha_2 = 116.9°$ and $\angle\ C_iN_{i+1}C_{i+1}^{\alpha} = \alpha_3 = 120.9°$ for the crystal structure, whereas the simulations give the following results: 110.1°, 116.9°, 120.0° (QMV(P)/MM(S)); 113.0°, 118.4°, 124.5° (MM, amber); 112.4°, 118.4°, 124.0° (MM, cedar); 112.5°, 116.4°, 123.7° (MM, charmm). The same simulation also results in moderate or high correlation with the crystal structure for the variations of these parameters along the peptide chain. The correlation is highest for bond angle α_1, where the correlation coefficient is 0.85. The two dihedral angles shown in Figure 1(c) represent deviations from planarity of the peptide units, and for these the correlation coefficients are 0.58 and 0.55, respectively. One can see that the MM simulations falsely predict these peptide bond dihedral angles to be secondary structure dependent, i.e., slightly but systematically away from 180° in the two α-helix regions, which are from residue Ile7 to Leu18 and from Glu23 to Thr30.

The closer agreement between the QMV(P)/MM(S) simulation and the 0.54 Å crystal structure is not a result of different peptide flexibility produced by the QM and MM models. The SCC-DFTB model in general produces higher flexibility than the MM models. This is shown by the largest average instantaneous RMS deviation produced by the QMV(P)MM(S) simulation (Table I). Other indicators such as RMS fluctuations of atomic positions in the simulations give the same result. Thus, the closer correlation cannot be explained by assuming that the QMV(P)/MM(S) simulation underestimates the flexibility of the protein.

DISCUSSION

Quantum mechanical calculations on crambin have been reported by Van Alsenoy et al.[25] Starting from a crystal structure, in vacuum geometry optimizations were performed for some steps, and the resulting structure were compared with the starting structure. The ab initio model used by these authors disallows for more extensive sampling in the conformational space. Solvent effects have also not been included in this study. Our current study goes beyond the static structure of crambin and focuses on dynamic aspects.

Comparisons between the QMV(P)/MM(S) and the QM(P)/MM(S) simulations reveal the critical role of the van der Waals interactions in stabilizing the native structure. This dynamic instability would not have been observed with energy minimization or very short (<10 ps) molecular dynamics simulations, where only local conformations very close to the starting structure can be explored.

The quantum mechanical simulation provides an opportunity to reevaluate some of the basic assumptions embedded in popular MM models of biopolymers. These include the assumptions of fixed atomic charge and of zero or unit charge per monomer in nonpolarizable models, and of limited, local redistribution of charge in polarizable dipole models. Indeed, the QMV(P)/MM(S) simulation produces significant instantaneous fluctuations, ≈10% of atomic charges, as shown for the backbone atoms in Figure 2(a). The same figure also shows that despite these large instantaneous fluctuations, the time-averaged atomic charges and their variations along the peptide chain are highly reproducible. Current fixed atomic charge models omit both the instantaneous charge fluctuations and the charge variations with protein environment. The simulation also shows that the neutral or unit-charge monomer assumption holds for most of the residues [see Fig. 2(b)]. However, notable exceptions are the C-terminal Asn46 with an averaged total charge of −0.75 e, and the N-terminal Thr1 with an averaged total charge of +0.83 e. The charge deficit at Cys4 of −0.13 e approximately accounts for the resulting residual part. These deviations

of monomer charges, as shown in Figure 2(c), cannot be captured by a fixed charge model and also not by a polarizable model with fluctuating dipoles.

Recently, Nadig and coworkers[26] reported divide-and-conquer semiempirical molecular orbital theory calculations on protein/water systems, in which they found significant charge-transfer interactions across the protein/water surface. It will be worth investigating if these occur also when the SCC-DFTB method is applied to both crambin molecule and solvent.

The nonlocal charge redistribution observed in our calculation may play a role in stabilizing the native three-dimensional fold of crambin. It seems to be associated with a group of residues (the N and C terminals, Thr2, Cys4, Arg10, and Phe13) that interact closely in space in the native fold and are conserved or only replaced by residues with the same functional groups in both sequence and fold of two proteins homologous to crambin, viscotoxin a3, and β-purothionin.[27]

In summary, we have constructed a general quantum mechanical-based approach with demonstrated accuracy toward long-time molecular dynamics simulation of proteins.

Our results highlight the importance of long-range van der Waals forces in quantum mechanical description of proteins. All current quantum mechanical methods potentially applicable to molecular dynamics simulation of large biological systems neglect the long-range van der Waals energy. Our results show that in quantum mechanical molecular dynamics simulation of biological systems, the weak van der Waals interactions must be included, either empirically, as in this work, or through more accurate quantum mechanical methods, which remains a challenge.

Our simulations of crambin show significant differences between the quantum mechanical and molecular mechanical descriptions of proteins. This development opens a wide range of possibilities for the investigation of chemical processes in biological systems.

ACKNOWLEDGMENTS

We thank North Carolina Supercomputer Center for providing the computer resource and Professor Ponder for use of his Tinker molecular modeling package in part of the work. HY Liu thanks Geoffrey Mann for his help with the molecular mechanics simulations.

REFERENCES

1. Karplus M, McCammon JA. Protein structural fluctuations during a period of 100 ps. Nature 1979;277:578.
2. Duan Y, Kollman PA. Pathways to a protein folding intermediate observed in a 1- microsecond simulation in aqueous solution. Science 1998;282:740–744.
3. Daura X, Gademann K, Jaun B, Seebach D, van Gunsteren WF, Mark AE. Peptide folding: when simulation meets experiment. Angew Chem Int Edit Eng 1999;38:236–240.
4. Warshel A, Levitt M. Theoretic studies of enzymic reactions: dielectric electrostatic and steric stabilization of the carbonium ion in the reaction of lysozyme. J Mol Biol 1976;103:227–249.
5. Field MJ, Bash PA, Karplus M. A combined quantum mechanical and molecular mechanical potential for molecular dynamics simulations. J Comput Chem 1990;11:700–733.
6. Gao J, Xia X. A priori evaluation of aqueous polarization effects through Monte Carlo QM-MM simulations. Science 1992;258:631–635.
7. Yang W, Lee T-S. A density-matrix divide-and-conquer approach for electronic structure calculations of large molecules. J Chem Phys 1995;163:5674–5678.
8. Yang W. Direct calculation of electron density in density-functional theory. Phys Rev Lett 1991;66:1438–1441.
9. Elstner M, Porezag D, Jungnickel G, Elstner J, Haugk M, Frauenheim T, Suhai S, Seifert G. Self-consistent-charge-density-functional tight-binding method for simulations of complex materials properties. Phys Rev 1998;B28:7260–7268.
10. Elstner M, Frauenheim T, Kaxiras E, Seifert G, Suhai S. A self-consistent charge density-functional based tight-binding scheme for large biomolecules. Phys Status Solidi B-Basic Res 2000;217:357–376.
11. Cornell WD, Cieplak P, Bayly CI, Gould IR, Merz KM, Ferguson DM, Spellmeyer DC, Fox T, Caldwell JW, Kollman PA. A second generation force field for the simulation of proteins, nucleic acids and organic molecules. J Am Chem Soc 1995;117:5179–5197.
12. Hermans J, Berendsen HJC, van Gunsteren WF, Postma JJP. A consistent empirical potential for water–protein interactions. Biopolymers 1984;23:1513–1518.
13. Ferro DR, McQueen JE, McCown JT, Hermans J. Energy minimizations of rubredoxin. J Mol Biol 1980;136:1–18.
14. MacKerell AD, Bashford D, Bellott MRL, Dunbrack J, Evanseck JD, Field MJ, Fischer S, Gao J, Guo H, Ha S, Joseph-MaCarthy D, Kuchnir L, Kuczera K, Lau FTK, Mattos C, Michnick S, Ngo T, Nguyen DT, Prodhom B, Reiher WE, Roux B, Schlenkrich M, Smith JC, Stote R, Straub J, Watanabe M, Wiorkiewicz-Kuczera J, Yin D, Karplus M. All-atom empirical potential for molecular modeling and dynamics studies of proteins. J Phys Chem 1998; B102:3586–3616.
15. Jelsch C, Teeter MM, Lamzin V, Pichon-Pesme V, Blessing RH, Lecomte C. Accurate protein crystallography at ultra-high resolution: Valence electron distribution in crambin. Proc Natl Acad Sci USA 2000;102:2246–2251.
16. Jorgensen WL, Chandrasekhar J, Madura J, Impey RW, Klein ML. Comparison of simple potential functions for simulating liquid water. J Chem Phys 1983;79:926–935.
17. Perdew JP, Chevary JA, Vosko SH, Jackson KA, Pederson MR, Singh DJ, Fiolhaise C. Atoms, molecules, solids and surfaces: Applications of the generalized gradient approximation for exchange and correlation. Phys Rev 1992;B46:6671–6687.
18. Porezag D, Frauenheim T, Köhler T, Seifert G, Kaschner R. Construction of tight-binding-like potentials on the basis of density-functional theory: Application to carbon. Phys Rev 1995;B58: 12947–12957.
19. Niehaus TA, Elstner M, Frauenheim TSS. Application of an approximate density-functional method to sulfur-containing compounds. J Mol Str (Theochem) 2001. Forthcoming.
20. Teeter MM, Roe SM, Heo NH. The high resolution (0.83 Å) crystal structure of the hydrophobic protein crambin at 130 K. J Mol Biol 1993;230:292–311.
21. Ryckaert JP, Ciccotti G, Berendsen HJC. Numerical integration of the Cartesian equations of motion of a system with constraints: Molecular dynamics of n-alkanes. J Comput Phys 1977;23:327–341.
22. van Gunsteren WF, Berendsen HJC, Colonna F, Perahia D, Hollenberg JP, Lellouch D. On searching neighbours in computer simulations of macromolecular systems. J Comput Chem 1984;5: 272–279.
23. Mooij WTM, van Duijneveldt FB, van Duijneveldt-van de Rijdt JGCM, van Eijck BP. Transferable ab initio intermolecular potentials. 1. Derivation from methanol dimer and trimer calculations. J Phys Chem 1999;A103:9872–9882.
24. Darden TA, York DM, Pedersen LG. Particle mesh Ewald: An N.log(N) method for Ewald sums in large systems. J Chem Phys 1993;98:10089–10092.
25. Van Alsenoy C, Yu C-H, Peeters A, Martin JML, Schäfer L. Ab initio geometry determinations in proteins. 1. Crambin. J Phys Chem 1998;102:2246–2251.
26. Nadig G, Van Zant LC, Dixon SL, Merz KM. Charge-transfer interactions in macromolecular systems: A new view of the protein/water interface. J Am Chem Soc 1998;120:5593–5594.
27. Whitlow M, Teeter MM. Energy minimization for tertiary structure prediction of homologous proteins-a-1-purothionin and viscotoxin-A3 models from crambin. J Biomol Struct Dyn 1985;2:831–848.